IEEE Access
Multidisciplinary ⋮ Rapid Review ⋮ Open Access Journal

Received February 24, 2019, accepted March 24, 2019, date of publication April 22, 2019, date of current version May 3, 2019.

Digital Object Identifier 10.1109/ACCESS.2019.2912650

Performance Comparison for Ballistocardiogram Peak Detection Methods

AHMAD SULIMAN[1], (Student Member, IEEE), CHARLES CARLSON[1], (Student Member, IEEE), CARL J. ADE[2], STEVE WARREN[1], (Member, IEEE), AND DAVID E. THOMPSON[1], (Member, IEEE)

[1]Department of Electrical and Computer Engineering, Kansas State University, Manhattan, KS 66506, USA
[2]Department of Kinesiology, Kansas State University, Manhattan, KS 66506, USA

Corresponding author: David E. Thompson (davet@ksu.edu)

This work was supported in part by the Kansas State University faculty startup funds, in part by the National Science Foundation General and Age-Related Disabilities Engineering (GARDE) Program under Grant CBET-1067740 and Grant UNS-1512564, and in part by the Kansas State University Open Access Publishing Fund.

ABSTRACT A number of research groups have proposed methods for ballistocardiogram (BCG) peak detection toward the identification of individual cardiac cycles. However, objective comparisons of these proposed methods are lacking. This paper, therefore, conducts a systematic and objective performance evaluation and comparison of several of these approaches. Five peak-detection methods (three replicated from the literature and two adapted from code provided by the methods' authors) are compared using data from 30 volunteers. A basic cross-correlation approach was also included as a sixth method. Two high-performing methods were identified: the method proposed by Sadek *et al.* and the method proposed by Brüser *et al.* The first achieved the highest average peak-detection rate of 94%, the lowest average false alarm rate of 0.0552 false alarms per second, and a relatively small mean absolute error between the real and detected peaks: 0.0175 seconds. The second method achieved the lowest mean absolute error of 0.0088 seconds between the real and detected peaks, an average peak-detection success rate of 89%, and 0.0766 false alarms per second. All metrics are averaged across participants.

INDEX TERMS Ballistocardiogram, heartbeat, heartbeat interval, heart rate, heart rate variability, load cells, statistical signal analysis, wavelets.

I. INTRODUCTION

Heart Rate (HR) and Heart Rate Variability (HRV) have proven to be useful for sleep staging [1]–[5] and other sleep quality assessments [6], [7]. HRV is used for long-term heart health monitoring and other clinical research [8], [9]. In [8], HRV is used to investigate relationships between cardiac autonomic modulations and breast cancer, and in [9], HRV is investigated as a subjective measure of well-being.

HRV assessment requires the identification of individual cardiac cycles toward the calculation of the times between every two consecutive heart beats. The time required for a heartbeat is often obtained, e.g., by identifying consecutive R peaks of an electrocardiogram (ECG) or consecutive peaks of a photoplethysmogram (PPG). These methods of heartbeat detection require the user to wear electrodes or a finger-mounted optical sensor, respectively. As a result, they are not ideal approaches for long-term monitoring.

Ballistocardiography, the measurement of micro-movements of the body due to blood ejection from the heart, is a promising alternative for pulse rate and HRV assessment. This general field has seen recent research interest [10] in terms of non-contact health monitoring, and a number of related peak detection and/or heartbeat interval estimation methods are proposed in the literature [11]–[28].

A few studies have performed small-scale comparisons of peak detection methods. For example, [24] quotes the performance of seven existing methods and [29] compares methods intended for camera-based sensors. Several groups have compared their proposed approach with previous methods from their own or affiliated labs [20], [27], [30], [31]. The ''multi-method'' algorithm [14], which runs four peak-detection algorithms on a ballistocardiogram (BCG) segment and fuses results from the three best-performing methods,

The associate editor coordinating the review of this manuscript and approving it for publication was Shovan Barma.

2169-3536 © 2019 IEEE. Translations and content mining are permitted for academic research only.
Personal use is also permitted, but republication/redistribution requires IEEE permission.
See http://www.ieee.org/publications_standards/publications/rights/index.html for more information.

could be considered a comparison. However, it focuses on the overall performance of three fused methods as a single method. Finally, [32] compares the performance of the "Maximal Overlap Discrete Wavelet Transform (MODWT)" [27] with performances of three other signal processing techniques using the mean absolute error (MAE) between the resulting ECG-based and BCG-based pulse rates.

Based on this early review, a broad quantitative performance comparison of signal processing methods proposed by different research groups is lacking. Further, a consensus does not exist in this research community regarding which peak detection method best serves as a gold standard for performance comparisons. Such comparisons would be well served by (1) a common data set with which multiple methods could be tested and (2) access to original source code that would allow for accurate code replication. This paper proposes a framework where the performance of different BCG peak detection methods and their associated signal processing techniques can be objectively evaluated in terms of peak detection efficiency and sensitivity.

This work compares five BCG peak detection methods, where three are recreated from the literature [24], [25], [31] and two are adapted from original code [20], [27]. The original codes from the mentioned studies were modified to address differences in sensing methods and sampling frequencies. The authors recently conducted a pilot study involving five participants in [33] to compare three peak detection methods [20], [24], [31]. The present study extends that work to include the performance of two additional methods [25], [27], where data from total of 30 participants supplement the original data in [33]. For clarity in this paper, each of these five methods is referred to by the last name of the corresponding first author: Lee *et al.* [24], Lydon *et al.* [20], Brüser *et al.* [31], Alvarado-Serrano *et al.* [25] and Sadek *et al.* [27]. A simple technique based on cross correlation (XCOR) is also included as a baseline for comparison.

This work contributes

- a comparison of five peak-detection techniques applied to load-cell data,
- two proposed peak-detection methods for use in HRV applications,
- performance benchmarks for researchers who seek to improve peak-detection performance and/or develop new BCG peak-detection approaches, and
- a portfolio of replicated algorithms for the peak detection methods presented here.

An overview of the signal processing and peak detection approaches utilized here is provided in Section I of the supplemental material. The reader is encouraged to refer to the original work for further details. When possible, the authors have preserved the terms originally employed in each study.

The rest of this paper is organized as follows. The Methods section describes the participant demographics, data collection approach, and performance metrics. That section also details the algorithm comparisons, including parameter optimization steps. The Results section reports the outcomes of these comparisons, and the Discussion section comments on these results, the limitations of these analyses, and future work.

II. METHODS

A. DATA RECORDING

Thirty healthy volunteers participated in this study: fourteen male (ages 30.9 $\pm$ 6.3 years) and sixteen female (ages 46.0 $\pm$ 18.5 years). Participants provided informed consent, and the recording process was performed in accordance with Kansas State University Institutional Review Board protocol No. 9386. Each participant laid on their back on a full-size bed with a stiff mattress. BCGs were recorded using four Measurement Specialties FX1902 load cells positioned beneath the corner bedposts. The signal conditioning circuitry employed bandpass filters with corner frequencies of 0.05 and 35 Hz–these circuits are further described in [34]. ECGs were simultaneously recorded using a GE Datex-Ohmeda Cardiocap^{TM}/5 patient monitor. The conditioned BCGs and ECGs were digitized at 250 Hz using a National Instruments (NI) 9220 16-bit multichannel data acquisition system, and these data were transferred to a local PC with an NI 9184 Ethernet chassis controlled by a LabVIEW virtual instrument. Data were visually inspected, and segments corrupted by motion artifacts were removed prior to heartbeat interval identification. From that point, all available data were included in the study.

B. SIGNAL SOURCE SELECTION

For each participant, a signal quality index (SQI) [35] was calculated for each of the four BCG segments acquired from the load cells, and then the BCG segment with the highest SQI was selected. That segment was then preprocessed as specified in each peak-detection method's original paper. SQI calculation details are provided in Section IV of the supplemental material.

C. GROUND TRUTH PEAK LABELING

The most prominent BCG peaks, termed "J peaks," identify heartbeat times. Simultaneously-recorded ECG R peaks were used as visual aids to identify BCG J peaks (except for three participants for whom ECG was not available). Due to variability in R-to-I intervals [36], and consequently R-to-J intervals, automated ECG-based J-peak annotation was avoided. Instead, given labeling conventions as in [37], [38], and with R peaks as visual references, two sets of 100 consecutive J peaks from two separate two-minute-long BCG sections were visually identified and annotated for use as ground truth (GT) peaks. The first set was used to optimize each peak-detection method, and the second set was used to evaluate the method's performance. For the three BCG recordings where simultaneous ECG data were unavailable, only BCG sections with visually indisputable J peaks as depicted in Fig. 1 were included in the study.

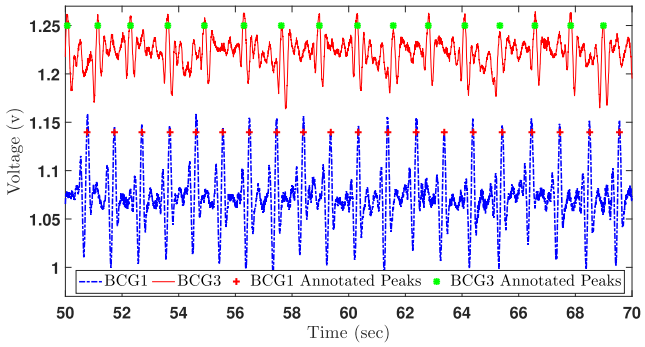

FIGURE 1. BCG excerpt with annotated J peaks for the 1st (bottom) and 3rd (top) participants for whom a simultaneous ECG was unavailable.

D. PERFORMANCE METRICS

A detection percentage (Det.) parameter is used as a sensitivity parameter to quantify the ability of an algorithm to correctly identify J peaks (i.e., a true positive rate). A false alarm rate (FAR) parameter represents the counter metric, or specificity. Any temporal shift introduced by a signal processing step was corrected so that the detected peaks in the BCG segment would align in time with their corresponding GT peaks. A detection, or true positive (TP), is defined as a detected peak that is within $d = 0.06$ sec of the GT peak [33]. While Šprager and Zazula [14] suggest 0.075 sec instead, this stricter criteria improves specificity and exceeds the IEC standard for ECG QRS detection used in [14]. If multiple peaks are detected within a target window, the positive peak closest to the GT peak is considered a TP, and the rest are counted as false positives (FPs). Likewise, peaks detected outside of the specified window are considered FPs. Unsuccessful detection within the target window near the GT peak is counted as a missed event or false negative (FN). The FAR is then defined as the number of all FP events between the first and last GT peaks divided by the time between the first and last GT peaks in seconds and is reported as counts/sec. The third metric considered in this study is the efficiency, r, as proposed in [14], which is defined in Eq. 1 as

$$r = \sqrt[3]{r_s \cdot r_p \cdot r_v} \tag{1}$$

where r_s and r_p represent sensitivity and precision, respectively, and r_v is the variability score. These parameters are defined in [14] as

$$r_s = \frac{\mathrm{TP}}{\mathrm{TP} + \mathrm{FN}}, \tag{2}$$

$$r_p = \frac{\mathrm{TP}}{\mathrm{TP} + \mathrm{FP}}, \tag{3}$$

and

$$r_v = P\big(\big|t_{d_i} - \big(t_{r_i} + \bar{\tau}\big)\big| < d\big), \tag{4}$$

where P is the probability, t_{d_i} and t_{r_i} are the i^{th} time indices of the detected and GT peaks, respectively, and $\bar{\tau}$ is the average time between detected and GT peaks if R peaks are used as GT peaks [14]. Since visually annotated J peaks are used as GT peaks, $\bar{\tau}$ is dropped and Eq. 4 becomes

$$r_v = P\big(\big|t_{d_i} - t_{r_i}\big| < d\big) \tag{5}$$

Looking at Eqs. 2 and 5, however, one can see that Eq. 5 is numerically equivalent to Eq. 2, i.e., $r_v = r_s$, and therefore a modified definition for r_v is considered in this work to avoid duplication in Eq. 1. The modified definition proposed here is the ratio of the number of detections within $d/2$ to the number of detections within d:

$$r_{v_{mod}} = \frac{P\big(\big|t_{d_i} - t_{r_i}\big| < d/2\big)}{r_v} = \frac{P\big(\big|t_{d_i} - t_{r_i}\big| < d/2\big)}{r_s} \tag{6}$$

which leads to

$$r_{mod} = \sqrt[3]{r_s \cdot r_p \cdot r_{v_{mod}}}, \tag{7}$$

and the efficiency for each method is computed using Eq. 7 instead of Eq. 1.

The fourth proposed metric is the MAE between the GT peak times and the detected peak times (MAE_p). This metric provides insight into J peak temporal jitter. The last performance measure is the *Absolute Error (AbsErr)* between each HBI based on GT peaks (HBI_{GT}) and each HBI based on detected J peaks (HBI_{det}). It is calculated using Eq. 8. Here, n is the total number of HBIs based on detected peaks from all participant BCGs.

$$AbsErr_n = \big|HBI_{GT_n} - HBI_{det_n}\big| \tag{8}$$

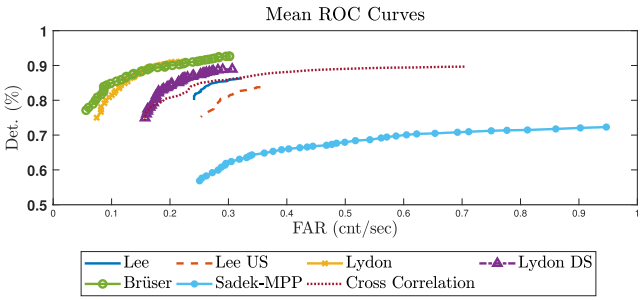

FIGURE 2. Mean ROC curves for the Lee, Lee-US, Lydon, Lydon-DS, Brüser, Sadek-MPP and XCOR methods. The -DS & -US methods are down- or up-sampled to match the original publication.

E. PARAMETER SELECTION AND OPTIMIZATION

Authors of some papers that present peak-detection methods either do not report one or more parameters, or the reported parameters lead to non-optimal performance when utilized with these BCG datasets. Reporting poor performance for a method would be arguably unfair if a simple parameter change would have made it competitive. Therefore, when replicating or adapting each method, the authors had to first optimize the method's performance by varying parameter values. To that end, a range of parameter values were iterated to obtain a set of Det. and FAR pairs for each method when applied to the first segment of a BCG with its associated GT peaks. The obtained Det. and FAR pairs were used to create receiver operating characteristic (ROC) curves. Parameter values were selected to maximize the area under the curve (AUC) for each of the ROC curves (see Fig. 2).

The plots include only the ROC curves for those methods that were able to produce smooth curves for detection rates above 65%. The factors limiting the depiction of ROC curves to detection rates above 65%, and only for certain methods, are discussed in IV-A and IV-D, respectively.

Since the Lee and Lydon methods were originally tested on BCGs sampled at 1000 and 100 Hz, respectively, an up-sampled and down-sampled BCG were utilized in this work in addition to direct application on our 250 Hz data. These two scenarios are labeled "Lee-US" (up-sampled BCG) and "Lydon-DS" (down-sampled BCG). This step was taken to rule out the effects of a sampling frequency mismatch. The same approach was applied with the Alvarado and Sadek methods, but it led to incomparable performances, so the results were not reported. For the Sadek method, a "minimum peak prominence" (MPP) parameter was evaluated in addition to the original "minimum peak distance" (MPD) parameter utilized with the MATLAB "findpeaks()" function. This scenario was labeled "Sadek-MPP" and was included in the results as a comparable method to the other methods that used MPP.

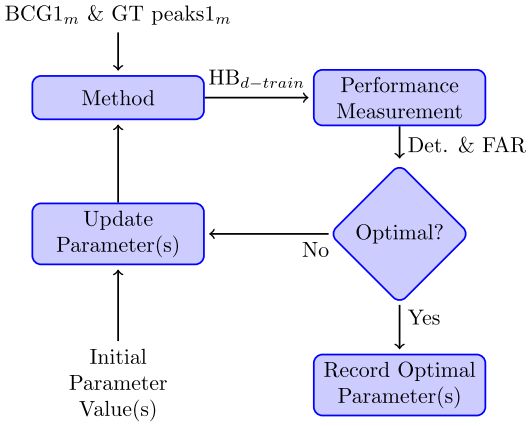

FIGURE 3. Performance optimization process. The path labeled "HB$_{d-train}$" indicates the detected heartbeats used to train the parameters to optimize the performance of a method.

The optimization process is illustrated by the flowchart in Fig. 3. BCG1$_m$ is the first two-minute-long BCG segment from the mth participant, including its associated GT peaks (GT peaks1$_m$); the result from that segment is detected heartbeats (HB$_d$). The parameter(s) noted in the flow chart are summarized in Table 1.

The rationale for picking these parameters and the other details of the optimizations are provided in Section II of the supplemental material. Also, a summary of the wavelet basis functions and the number of participants for whom these functions resulted in an optimal performance (with the Alvarado and Sadek methods) are provided in Tables 1 and 2, respectively, in section III of the supplemental material.

F. TESTING PHASE

After the parameters were optimized, performance metrics were computed when using the second BCG segment, BCG2$_m$, and its associated GT peaks, GT peaks2$_m$.

TABLE 1. List of parameters to be optimized for each method.

Method	Parameters Used
Lee, Lydon, XCOR	Moving-average Lengths
Lee, Lydon, XCOR, Sadek	"Minimum peak prominence" (MPP)
Brüser	Sliding window overlap percentage, th_Q
Alvarado	Wavelet basis function; Wavelet decomposition level
Sadek	Wavelet decomposition level; "minimum peak distance" (MPD); "Analysis Window" size

TABLE 2. Performance metrics for the various peak-detection methods. Det.: detection rate in %, FAR: False Alarm Rate in alarms per second (cnt/sec), MAE$_p$: Mean Absolute Error between GT peak times and detected J peak times in seconds, and r$_{mod}$: Efficiency in %.

Methods	Det. (%)	FAR (cnt/sec)	MAE$_p$ (sec)	r$_{mod}$ (%)
Lee	82.86	0.1047	0.0203	54.72
Lee-US	82.52	0.1028	0.0232	57.36
Lydon	86.35	0.0810	0.0175	66.06
Lydon-DS	81.52	0.0946	0.0184	60.84
Brüser	88.93	0.0766	0.0088	49.92
Alvarado	79.38	0.1714	0.0312	33.07
Sadek	94.17	0.0552	0.0175	44.97
Sadek-MPP	70.24	0.1920	0.0175	42.69
XCOR	89.17	0.1787	0.0103	52.37

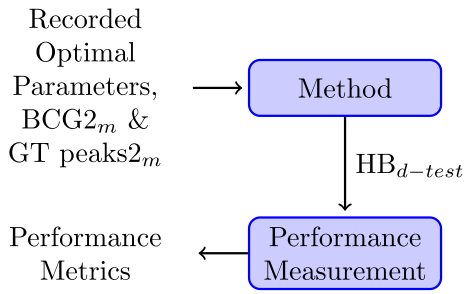

FIGURE 4. Performance evaluation based on the obtained parameters. The path labeled "HB$_{d-test}$" indicates the detected heartbeats used to test the performance of a method in conjunction with the parameters obtained in the optimization process, e.g., recorded optimal parameters.

These data were not used during the optimization process, so the peak-detection performance relative to these data should be a fair estimate of each method's ability. Fig. 4 illustrates this process further.

III. RESULTS

The performance metrics described in Section II-D are summarized in Table 2. The columns report averages taken across the number of participants: aggregate results for Det. in percent, FAR in counts per second, MAE$_p$ in seconds, and r$_{mod}$ in percent. Each row addresses a method noted in this paper.

The modified Bland-Altman plots in Figs. 5 and 6 display the HBI Error of each method on the dependent axis.

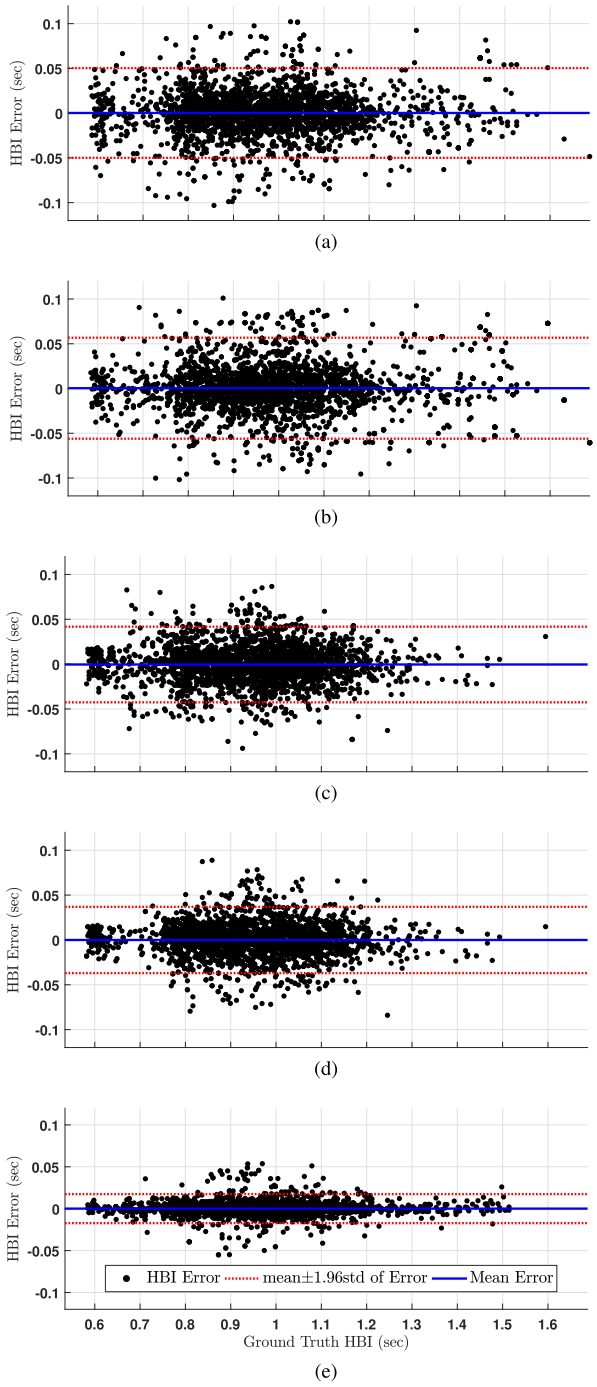

FIGURE 5. Modified Bland-Altman plots for the Lee, Lee-US, Lydon, Lydon-DS, and Brüser methods from top to bottom, respectively. (a) Lee. (b) Lee-US. (c) Lydon. (d) Lydon-DS. (e) Brüser.

The independent axis represents the HBI based on GT peaks as per recommendations in [39]. Each plot is based on aggregated HBI data for all 30 participants.

IV. DISCUSSION

A. LEE METHOD

The advantages of this method are its relatively low FAR and its low sensitivity to the sampling rate, as noted in Table 2 (the performance metrics are not much different for the Lee and Lee-US methods). This method also has the second highest efficiency (r_{mod}) for both sampling rates. The method's disadvantages are its relatively low detection power and its second-highest MAE_p. The Lee and Lee-US methods produce the most dispersed Bland-Altman plots (see the top two panels of Fig. 5). Lee's method as replicated in this work is also sensitive to parameter variations, and this sensitivity increases in the case of an up-sampled BCG.

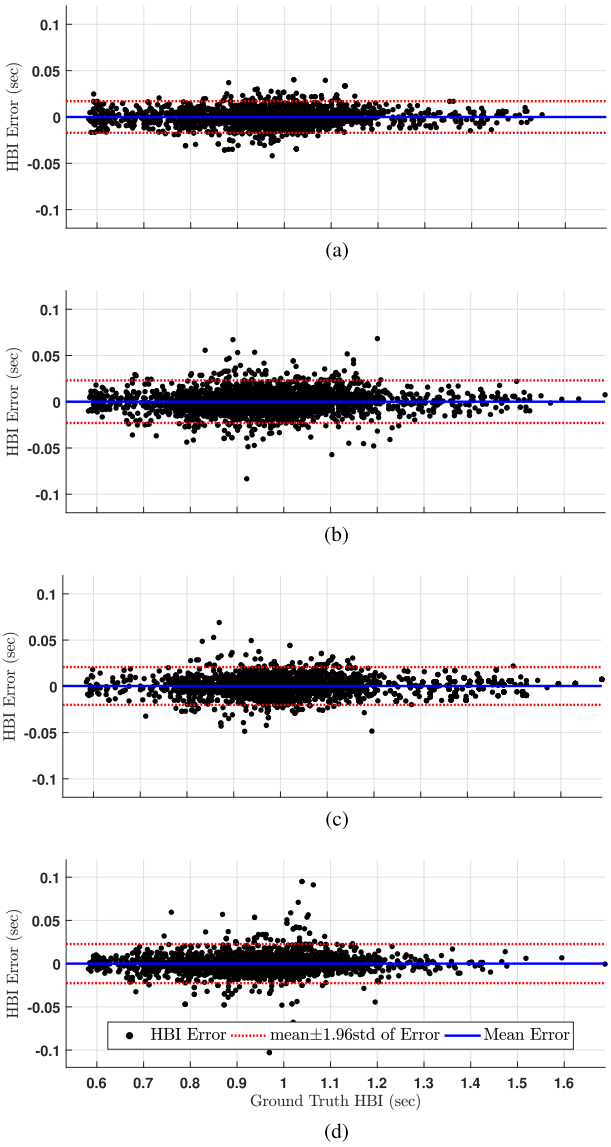

FIGURE 6. Modified Bland-Altman plots for the Alvarado, Sadek, Sadek-MPP, and XCOR methods from top to bottom, respectively. (a) Alvarado. (b) Sadek. (c) Sadek-MPP. (d) XCOR.

Since the next peak detection "analysis window" is based on the last peak detected in the previous window, it is not possible to create smooth ROC curves for larger ranges of the MPP values. Consequently, a complete ROC curve could not be produced during the optimization step. An example ROC curve for a wider range of MPP values is depicted in Fig. 7, where MPP was varied from 5e-4 to 10e-4 for participant 23. To address this issue, smaller ranges of parameter values were

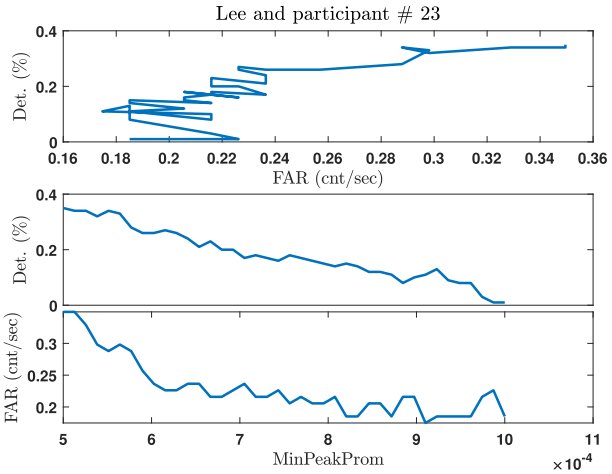

FIGURE 7. Top: ROC curve; Middle and bottom: Det. and FAR, respectively, vs minimum peak prominence (MPP) for a range of 5e-4 to 10e-4 for participant 23.

used to produce smooth ROC curve segments with detection rates exceeding 80% and FAR values below 0.2 cnt/sec. Exceptions were made for two participants because the parameter ranges needed to be as small as 2.2e-3 to 2.9e-3 in one case (participant number 6) and 3.2e-5 to 5e-5 in another case (participant number 3). Consequently, the Det. dropped to well below 80% and the effects were more pronounced in the Lee-US ROC curves, as can be seen in the second panel of Fig. 2. Similarly, for the Lee-US method applied to one participant's data, the FAR had to exceed 0.2 counts/sec to make a non-zero detection.

The method is prone to false positives introduced by end effects from filtering during each window. This problem can be alleviated by either performing preprocessing prior to windowing or by introducing an MA filter on the output. The latter was chosen but led to two MA length parameters that required optimization. Contrary to the initial study [33], performance was substantially improved by setting this second parameter in a subject-specific manner.

B. LYDON METHOD

The advantages of this method are that it offers the highest r_{mod}, the third lowest FAR and MAE_p, and the easiest implementation after the XCOR method. The original code is also accessible. This method produced smooth ROC curves during the optimization process and was much less sensitive to variations in MPP values compared to the Lee method. The disadvantages of this method are its relatively low detection rate and the fact that it produces the second most dispersed Bland-Altman plots (3^{rd} and 4^{th} panels of Fig. 5). In addition, the existence of two lengths for the MA filters, which need to be adjusted for different participants, adds to its complexity for real-time peak detection. Comparing the two sampling rate scenarios for this method, an improved performance arises in the Lydon method when compared to the Lydon-DS approach. This can be due to distortion/loss of information from down-sampling the BCG or the notion that this method may perform better with BCGs recorded at higher sampling rates.

C. BRÜSER METHOD

The advantages of this method are that it has the lowest MAE_p, the second lowest FAR, and the third highest detection rate, plus it produces the second least dispersed Bland-Altman plot (see the 5^{th} panel in Fig. 5). This method is also less sensitive to parameter variations and produces good combinations of Det. and FAR for a larger range of parameter values. The ROC curves stay mostly near detection rates higher than 85%, with corresponding FARs as low as 0.07 counts/sec.

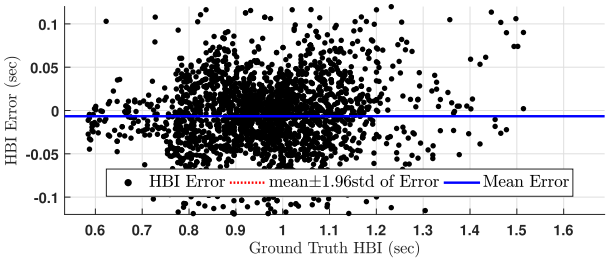

FIGURE 8. Modified Bland-Altman plot for the Brüser method when HBIs estimated by this method are used.

Interestingly, the version of Brüser's Method replicated for this work seems to produce better Bland-Altman plots when its detected peaks (''anchor points'' in the original work) are used instead of the directly estimated HBIs, although this method primarily focuses on direct HBI estimation. Fig. 8 displays the modified Bland-Altman plot obtained from the aggregate HBI estimates. The Bland-Altman plot in this figure is more dispersed when compared to the Bland-Altman plot for the Brüser method in Fig. 5. Also note that the ''mean±1.96std'' lines have moved outside of the limits (−0.1 to 0.1 on the dependent axis) used for Bland-Altman plots in this paper.

Since this study primarily focuses on peak-detection performance, including the Bland-Altman plots due to HBIs obtained from detected peaks should still be sensible. With a single subject-specific parameter to control, this method could be attractive for longitudinal peak detection applications.

A disadvantage of this method is that it has the third lowest r_{mod} after the Alvarado and Sadek methods based on the numbers in Table 2. The statistical approach taken in this method to determine HBI estimates makes this method more interesting for long-term longitudinal studies, since more personalized estimators can be trained and better decisions can be made when picking suitable HBIs. On the other hand, this same approach makes this method less attractive for short-term HRV estimation applications, since prior data must be accumulated to enhance the estimators used when picking good HBI estimates.

D. ALVARADO METHOD

The advantage of this method is that it offers subject-independent amplitude and interval thresholds, owing to the adaptive nature of its peak detection algorithm, as opposed to the ''findpeaks()'' algorithm used in the other methods (except for Brüser's method). Out of the six wavelet basis functions evaluated when optimizing this method, ''bior2.2'' resulted in the best performance for 13 BCGs. This suggests that it may be possible to deduce an optimal wavelet for a group of people with certain characteristics. This method also produces the least dispersed Bland-Altman plot: the 1^{st} panel in Fig. 6. The disadvantages of this method are that it produces the lowest r_{mod}, the lowest Det. after Sadek-MPP, the third highest FAR after XCOR and Sadek-MPP, and the highest MAE_p. Alvarado's method is also highly sensitive to wavelet decomposition scale selection in a non-linear fashion. For example, when changing from scale 68 to either 67 or 69 for a particular participant, the FAR will jump from zero to 0.66 or 0.63 counts/sec, respectively. Due to this non-linear sensitivity, a smooth ROC curve was not possible.

For the BCG data employed here, the originally-proposed 5^{th} decomposition level performed poorly, yielding an average detection rate of 27% and 0.89 counts/sec FAR. Different wavelet decomposition scales were therefore investigated. The best-performing scales were often much higher (between 19 and 76).

E. SADEK METHOD

For Sadek's method, the Sadek and Sadek-MPP implementations will be discussed separately. The advantages of the Sadek algorithm are that it offers the highest detection rate, the lowest FAR, and the third lowest MAE_p, plus it produces the third least dispersed Bland-Altman plot (panel two in Fig. 6). This method is also attractive because the code is publicly accessible. One disadvantage is that this method produces the third lowest r_{mod}. It also needs prior HBI data from a participant for proper ''minimum peak distance'' (MPD) selection, making short-term HRV studies impossible. In addition, this method lacks a means to find an optimal MPD value in the long run. Brüser's method, for instance, handles this automatically using statistical estimators. Because this parameter is fixed, the Sadek method may not be suitable for long-term or longitudinal studies due to changes in the underlying heart rate.

The advantage of the Sadek-MPP method is that it can be used for long-term longitudinal HRV studies, because once an optimal MPP is obtained, the MPP will not change unless the participant changes. The method's less dispersed Bland-Altman plot can be an advantage but is misleading due to the low number of detections obtained with this method; Bland-Altman plots do not account for misses. Other disadvantages of this method are that it offers the highest FAR, the lowest Det., the second-lowest r_{mod}, and a relatively high MAE_p.

The wavelet proposed in the original work, ''sym8'', appears to result in better performance for both the Sadek and Sadek-MPP methods when applied to these participant data. The wavelet decomposition scales do not vary significantly, and a wavelet decomposition scale of 6 seems to produce optimal results for 17 participants. This implies the possibility to identify a subject-independent scale for a group of individuals who share similar physiological and body composition traits. Note, though, that transitioning from the optimal scale to the neighboring scale impacts the performance severely. For example, a transition from scale 5 to scale 6 for participant 8 causes the detection rate to drop from 100 % to 32% and the FAR to increase from 0 to 0.64 counts/sec.

In this method, similar results are obtained whether or not windowing is applied. However, if windowing is applied, a 10-second window length as proposed in the original work is not always optimal. While the authors applied the windowing step when using an MPD to be consistent with the original work, this step was skipped when using an MPP. This can be justified because when windowing is applied after wavelet decomposition, end effects will not exist for each window and therefore will not affect the performance of the method. Also, the MATLAB ''findpeaks()'' function applies windowing anyway, which partly explains why windowing does not affect performance in the first place.

Down-sampling these BCG data to the originally proposed sampling rate (50 Hz) severely impacts the performance of this method. For example, the average Det. drops to 13% and the average FAR jumps to 0.8855 counts/sec when tested with an MPD. Based on this observation, the Sadek-MPP method was not tested with a down-sampled BCG. Consequently, results for down-sampled data were not considered in the evaluation process.

F. CROSS-CORRELATION METHOD

The advantages of this method are that it offers the second highest detection rate, the second lowest MAE_p, a relatively high r_{mod}, and minimal design complexity. The performance of this method is much less sensitive to parameter variations when compared to methods that use MPPs. As a result, it provides a larger range of parameter variations toward smoother ROC curves. As mentioned in the Methods section, the lengths of the MA filters were subject-independent except for the case of one participant whose data were later removed from the study since they caused this method to produce zero Det./FAR pairs. The disadvantages of this method are that its FAR is the second highest, and it produces a relatively more dispersed Bland-Altman plot-see panel four in Fig. 6. The fact that it failed to find a non-zero Det./FAR pair for the BCG of a particular participant is another negative point, although those BCG data caused the Lee and Lydon methods to perform poorly as well.

G. LIMITATIONS

While considerable effort has been expended to accurately replicate each method, the possibility of error remains. Original code was not available from most of the affiliated authors (except for the authors of [20] and [27]), and some details necessary to replicate the methods were missing from each paper.

Therefore, it is sensible to note that the results presented in this study relate to the performance of the authors' *replications* of each method. The parameter optimization process was included to mitigate the effects caused by inconsistencies in method implementations relative to the algorithms created for the original papers.

An occasional small modification was necessary to avoid unfairly penalizing a given method. For example, a simple MA filter was added to the Lee and Lydon methods, since their performance would otherwise have been very poor. Some parameters either were not listed in the original publications or were obviously inappropriate for these BCG data; these parameters were adjusted through the parameter optimization step described earlier. For many parameters, though, the published values were used directly without investigating other settings. Notably, the filter types, orders, and corner frequencies were implemented as published. Optimizing these parameters may have led to increased performance for some methods, but doing so would substantially increase the complexity of the optimization. While some methods originally included an automatic motion artifact removal step, that step was skipped in this study since the BCG segments selected for this work were already free of motion artifact.

As mentioned in the Methods section, BCG selection (i.e., one signal out of four available load cell signals) was based on the signal with the highest SQI. While this step was performed with the goal to select the best BCG, a higher SQI did not necessarily result in better algorithm performance. Nonetheless, the performance comparison is still reasonable, since the same BCG data were presented to all methods.

The overall low r_{mod} as noted in Table 2 is due to the $r_{v_{mod}}$ factor in Eq. 7, which is defined in Eq. 6. Eq. 6 is relatively strict at present. Ultimately, however, the research goal is to place limits on the HRV estimate error rather than the time-domain jitter. Further study will be required to elucidate this relationship.

A Bland-Altman plot compares only one performance aspect: the error between a GT value and an estimate. Since false alarm events are ignored, similar plots can be obtained for two methods with similar jitters but very different Det. and FAR values. The authors therefore suggest that Bland-Altman plots are suitable but not fully sufficient for this type of method comparison.

Since the BCG ground truth peaks were not based on the R peaks of ECG data, the mean relative error between the R-to-R intervals (RRIs) and the heartbeat intervals (HBIs) [40] was not used as a performance criterion in this work. Here, the authors believe that MAE_p is a good replacement for this measure.

H. FUTURE WORK

The role of sensor modality is unclear in terms of performance differences between these peak-detection methods. The Lee method was originally proposed for use with load cell data, consistent with this work. Lydon *et al.* used water pressure sensors in their original work, but the Lydon method can clearly be successfully used with load cell-based BCGs, since Lydon's method outperformed Lee's method in this study. Similarly, Brüser's method, though originally designed for data acquired with electromechanical films, had a high number of detections and a low timing jitter. This suggests that Brüser's method may be more robust to sensor changes than the other techniques. On the contrary, the Alvarado and Sadek-MPP methods, originally proposed for fiber-optic based sensors, performed poorly. Perhaps the sensor modality mismatch is one reason. Further study is needed.

The existence of at least one subject-dependent parameter for each method suggests that these methods will achieve their best performance in long-term and longitudinal studies only if the parameters are personalized for each user. Since each data set for this study originated from a single session, the authors cannot speak to the stability of these parameters over time.

In this study, a timing jitter up to 0.06 sec (when comparing a candidate peak to a GT peak) resulted in the tally of a detected peak. However, it is not yet clear how much timing jitter can be allowed before an HRV feature estimated using these detected peaks will become useless. Further studies are necessary to assess the impact of timing jitter on the quality of the HRV features.

As mentioned earlier, the results of this study are based on BCGs with no motion artifacts. When processing longer BCG segments, where motion artifacts are unavoidable, an automatic motion detection algorithm such as in [41] may prove useful. The preferred peak-detection method as identified by this work can then be applied to the remaining clean BCG data.

BCGs are not the only unobtrusive signals used for heartbeat detection. Several other non-contact heartbeat detection methods have been proposed in the literature, such as capacitive ECGs [42]–[47], mattress-based PPGs [48], PPG imaging [49]–[54], optical Doppler or laser-based techniques (e.g., for tracking the cardiac chamber or arterial wall movements) [55]–[60], thermography [61]–[64], video-based motion analysis [65], [66] (see [29] for a thorough review), and high frequency electromagnetic fields [67]–[71] (see [72] for a review and elaboration of some of these approaches). The platform developed for this work may show promise when comparing the performance of heartbeat detection methods applied to data acquired using these other sensing modalities.

V. CONCLUSION

This paper compared the peak-detection performance of various algorithms when applied to ballistocardiographic data acquired from load cells placed under the corner posts of a bed. No single method excelled in all comparison categories. However, Brüser's method had the lowest timing jitter, the second lowest false alarm rate, and the third highest detection power. Sadek's method also exhibited good performance, offering the highest detection power, the lowest false alarm rate, and the third lowest timing jitters; it would be a strong

candidate if not for its high dependence on the ''minimum peak distance'' parameter, which requires prior knowledge of an individual's heartbeat interval. On the other hand, Sadek's method does have a subject-independent wavelet basis function which would be desirable if a robust scheme to train the ''minimum peak distance'' could be developed. Interestingly, the simple XCOR method presented by the authors would be in third place, as it yielded the second highest detection power and the second lowest timing jitter. However, the high false alarm rate reported by this method requires attention. The code that implements the framework proposed in this study is accessible upon request to the corresponding author. A link to Code Ocean repository will be available in the future.

ACKNOWLEDGMENTS

Opinions, findings, conclusions, or recommendations expressed in this material are those of the authors and do not necessarily reflect the views of the funding agencies. Human subjects work affiliated with this research was approved by the Kansas State University Institutional Review Board under protocol No. 9386. The authors acknowledge and appreciate the cooperation of Dr. Skubic and her team, as well as Dr. Mokhtari and his team, for providing the original code for the Lydon and Sadek methods, respectively.

REFERENCES

[1] E. Yuda, Y. Yoshida, R. Sasanabe, H. Tanaka, T. Shiomi, and J. Hayano, ''Sleep stage classification by a combination of actigraphic and heart rate signals,'' *J. Low Power Electron. Appl.*, vol. 7, no. 4, p. 28, 2017.

[2] J. Hayano, E. Yuda, and Y. Yoshida, ''Sleep stage classification by combination of actigraphic and heart rate signals,'' in *Proc. IEEE Int. Conf. Consum. Electron.-Taiwan (ICCE-TW)*, Jun. 2017, pp. 387–388.

[3] S. Nurmi, T. Saaresranta, T. Koivisto, U. Meriheinä, and L. Palva, ''Validation of an accelerometer based BCG method for sleep analysis,'' Aalto Univ., Helsinki, Finland, Tech. Rep., 2016. [Online]. Available: https://aaltodoc.aalto.fi:443/handle/123456789/21176

[4] H. Ni, T. Zhao, X. Zhou, Z. Wang, L. Chen, and J. Yang, ''Analyzing sleep stages in home environment based on ballistocardiography,'' in *Proc. Int. Conf. Health Inf. Sci.* Cham, Switzerland: Springer, 2015, pp. 56–68.

[5] M. Xiao, H. Yan, J. Song, Y. Yang, and X. Yang, ''Sleep stages classification based on heart rate variability and random forest,'' *Biomed. Signal Process. Control*, vol. 8, no. 6, pp. 624–633, 2013.

[6] Z. Dong, X. Li, and W. Chen, ''Frequency network analysis of heart rate variability for obstructive apnea patient detection,'' *IEEE J. Biomed. Health Inform.*, vol. 22, no. 6, pp. 1895–1905, Nov. 2018.

[7] D. W. Jung, S. H. Hwang, H. N. Yoon, Y.-J. G. Lee, D.-U. Jeong, and K. S. Park, ''Nocturnal awakening and sleep efficiency estimation using unobtrusively measured ballistocardiogram,'' *IEEE Trans. Biomed. Eng.*, vol. 61, no. 1, pp. 131–138, Jan. 2014.

[8] C. Arab *et al.*, ''Cardiac autonomic modulation impairments in advanced breast cancer patients,'' *Clin. Res. Cardiol.*, vol. 107, no. 10, pp. 924–936, 2018.

[9] K. Boman, ''Heart rate variability: A possible measure of subjective well-being?'' Univ. Skövde, School Bioscience, Skövde, Sweden, Tech. Rep., 2018.

[10] X. Feng, Y. Xu, M. Dong, and P. Levy, ''Non-contact home health monitoring based on low-cost high-performance accelerometers,'' in *Proc. 2nd IEEE/ACM Int. Conf. Connected Health, Appl., Syst. Eng. Technol.*, Jul. 2017, pp. 356–364.

[11] J. M. Kortelainen and J. Virkkala, ''FFT averaging of multichannel BCG signals from bed mattress sensor to improve estimation of heart beat interval,'' in *Proc. 29th Annu. Int. Conf. IEEE Eng. Med. Biol. Soc.*, Aug. 2007, pp. 6685–6688.

[12] D. C. Mack, J. T. Patrie, P. M. Suratt, R. A. Felder, and M. Alwan, ''Development and preliminary validation of heart rate and breathing rate detection using a passive, ballistocardiography-based sleep monitoring system,'' *IEEE Trans. Inf. Technol. Biomed.*, vol. 13, no. 1, pp. 111–120, Jan. 2009.

[13] J. M. Kortelainen, M. O. Mendez, A. M. Bianchi, M. Matteucci, and S. Cerutti, ''Sleep staging based on signals acquired through bed sensor,'' *IEEE Trans. Inf. Technol. Biomed.*, vol. 14, no. 3, pp. 776–785, May 2010.

[14] S. Sprager and D. Zazula, ''Heartbeat and respiration detection from optical interferometric signals by using a multimethod approach,'' *IEEE Trans. Biomed. Eng.*, vol. 59, no. 10, pp. 2922–2929, Oct. 2012.

[15] C. Brüser, S. Winter, and S. Leonhardt, ''Unsupervised heart rate variability estimation from ballistocardiograms,'' in *Proc. 7th Int. Workshop Biosignal Interpretation*, 2012, pp. 1–6.

[16] C. Brüser, S. Winter, and S. Leonhardt, ''How speech processing can help with beat-to-beat heart rate estimation in ballistocardiograms,'' in *Proc. IEEE Int. Symp. Med. Meas. Appl. (MeMeA)*, May 2013, pp. 12–16.

[17] A. Vehkaoja, S. Rajala, P. Kumpulainen, and J. Lekkala, ''Correlation approach for the detection of the heartbeat intervals using force sensors placed under the bed posts,'' *J. Med. Eng. Technol.*, vol. 37, no. 5, pp. 327–333, 2013.

[18] Y. Yao, C. Bruser, U. Pietrzyk, S. Leonhardt, S. van Waasen, and M. Schiek, ''Model-based verification of a non-linear separation scheme for ballistocardiography,'' *IEEE J. Biomed. Health Inform.*, vol. 18, no. 1, pp. 174–182, Jan. 2014.

[19] Y. Yao, J. Schiefer, S. van Waasen, and M. Schiek, ''A non-parametric model for Ballistocardiography,'' in *Proc. IEEE Workshop Stat. Signal Process. (SSP)*, Jun./Jul. 2014, pp. 69–72.

[20] K. Lydon *et al.*, ''Robust heartbeat detection from in-home ballistocardiogram signals of older adults using a bed sensor,'' in *Proc. 37th Annu. Int. Conf. IEEE Eng. Med. Biol. Soc. (EMBC)*, Aug. 2015, pp. 7175–7179.

[21] I. Sadek, J. Biswas, V. F. S. Fook, and M. Mokhtari, ''Automatic heart rate detection from FBG sensors using sensor fusion and enhanced empirical mode decomposition,'' in *Proc. IEEE Int. Symp. Signal Process. Inf. Technol. (ISSPIT)*, Dec. 2015, pp. 349–353.

[22] M. Krej, Ł. Dziuda, and F. W. Skibniewski, ''A method of detecting heartbeat locations in the ballistocardiographic signal from the fiber-optic vital signs sensor,'' *IEEE J. Biomed. Health Inform.*, vol. 19, no. 4, pp. 1443–1450, Jul. 2015.

[23] J. Paalasmaa, H. Toivonen, and M. Partinen, ''Adaptive heartbeat modeling for beat-to-beat heart rate measurement in ballistocardiograms,'' *IEEE J. Biomed. Health Inform.*, vol. 19, no. 6, pp. 1945–1952, Nov. 2015.

[24] W. K. Lee, H. Yoon, C. Han, K. M. Joo, and K. S. Park, ''Physiological signal monitoring bed for infants based on load-cell sensors,'' *Sensors*, vol. 16, no. 3, p. 409, Mar. 2016. [Online]. Available: http://www.mdpi.com/1424-8220/16/3/409

[25] C. Alvarado-Serrano, P. S. Luna-Lozano, and R. Pallàs-Areny, ''An algorithm for beat-to-beat heart rate detection from the BCG based on the continuous spline wavelet transform,'' *Biomed. Signal Process. Control*, vol. 27, pp. 96–102, May 2016.

[26] I. Sadek *et al.*, ''Sensor data quality processing for vital signs with opportunistic ambient sensing,'' in *Proc. 38th Annu. Int. Conf. IEEE Eng. Med. Biol. Soc. (EMBC)*, Aug. 2016, pp. 2484–2487.

[27] I. Sadek, J. Biswas, B. Abdulrazak, Z. Haihong, and M. Mokhtari, ''Continuous and unconstrained vital signs monitoring with ballistocardiogram sensors in headrest position,'' in *Proc. IEEE EMBS Int. Conf. Biomed. Health Inform. (BHI)*, Feb. 2017, pp. 289–292.

[28] I. Sadek, J. Bellmunt, M. Kodyš, B. Abdulrazak, and M. Mokhtari, ''Novel unobtrusive approach for sleep monitoring using fiber optics in an ambient assisted living platform,'' in *Proc. Int. Conf. Smart Homes Health Telematics*. Cham, Switzerland: Springer, 2017, pp. 48–60.

[29] A. Al-Naji, K. Gibson, S.-H. Lee, and J. Chahl, ''Monitoring of cardiorespiratory signal: Principles of remote measurements and review of methods,'' *IEEE Access*, vol. 5, pp. 15776–15790, 2017.

[30] L. R. Paniagua, ''Short-term heart rate variability as a general indicator of health estimated by ballisocardiography using a hydraulic bed sensor in elder care,'' Ph.D. dissertation, Dept. Elect. Eng., Univ. Missouri, Columbia, MO, USA, 2016.

[31] C. Brüser, S. Winter, and S. Leonhardt, ''Robust inter-beat interval estimation in cardiac vibration signals,'' *Physiol. Meas.*, vol. 34, no. 2, p. 123, 2013.

[32] I. Sadek and J. Biswas, ''Nonintrusive heart rate measurement using ballistocardiogram signals: A comparative study,'' *Signal, Image Video Process.*, vol. 13, no. 3, pp. 475–482, 2018.

[33] A. Suliman, C. Carlson, S. Warren, and D. Thompson, ''Performance evaluation of processing methods for ballistocardiogram peak detection,'' in *Proc. 40th Annu. Int. Conf. IEEE Eng. Med. Biol. Soc. (EMBC)*, Jul. 2018, pp. 502–505.

[34] C. Carlson *et al.*, "Bed-based instrumentation for unobtrusive sleep quality assessment in severely disabled autistic children," in *Proc. 38th Annu. Int. Conf. IEEE Eng. Med. Biol. Soc. (EMBC)*, Aug. 2016, pp. 4909–4912.
[35] A. O. Bicen and O. T. Inan, "A signal quality index for ballistocardiogram recordings based on electrocardiogram RR intervals and matched filtering," in *Proc. IEEE EMBS Int. Conf. Biomed. Health Inform. (BHI)*, Mar. 2018, pp. 145–148.
[36] X. Zhang, L. Zhang, K. Wang, C. Yu, T. Zhu, and J. Tang, "A rapid approach to assess cardiac contractility by ballistocardiogram and electrocardiogram," *Biomed. Eng./Biomedizinische Technik*, vol. 63, no. 2, pp. 113–122, 2016.
[37] I. Starr, A. Rawson, H. A. Schroeder, and N. Joseph, "Studies on the estimation of cardiac ouptut in man, and of abnormalities in cardiac function, from the heart's recoil and the blood's impacts; the ballistocardiogram," *Amer. J. Physiol.-Legacy Content*, vol. 127, no. 1, pp. 1–28, 1939.
[38] W. R. Scarborough *et al.*, "Proposals for ballistocardiographic nomenclature and conventions: Revised and extended: Report of committee on ballistocardiographic terminology," *Circulation*, vol. 14, no. 3, pp. 435–450, 1956.
[39] J. S. Krouwer, "Why bland–altman plots should use X, not (Y+X)/2 when X is a reference method," *Statist. Med.*, vol. 27, no. 5, pp. 778–780, 2008.
[40] C. Brüser, J. M. Kortelainen, S. Winter, M. Tenhunen, J. Pärkkä, and S. Leonhardt, "Improvement of force-sensor-based heart rate estimation using multichannel data fusion," *IEEE J. Biomed. Health Inform.*, vol. 19, no. 1, pp. 227–235, Jan. 2015.
[41] A. Alivar *et al.*, "Motion artifact detection and reduction in bed-based ballistocardiogram," *IEEE Access*, vol. 7, pp. 13693–13703, 2019.
[42] H. J. Lee, S. M. Lee, K. M. Lee, and K. S. Park, "Performance evaluation of electrocardiogram measured using capacitive textiles on a bed," in *Proc. BIODEVICES*, 2011, pp. 436–439.
[43] K.-F. Wu and Y.-T. Zhang, "Contactless and continuous monitoring of heart electric activities through clothes on a sleeping bed," in *Proc. Int. Conf. Inf. Technol. Appl. Biomed. (ITAB)*, 2008, pp. 282–285.
[44] Y. G. Lim, K. K. Kim, and K. S. Park, "ECG recording on a bed during sleep without direct skin-contact," *IEEE Trans. Biomed. Eng.*, vol. 54, no. 4, pp. 718–725, Apr. 2007.
[45] Y. G. Lim *et al.*, "Monitoring physiological signals using nonintrusive sensors installed in daily life equipment," *Biomed. Eng. Lett.*, vol. 1, no. 1, pp. 11–20, 2011.
[46] M. Ishijima, "Monitoring of electrocardiograms in bed without utilizing body surface electrodes," *IEEE Trans. Biomed. Eng.*, vol. 40, no. 6, pp. 593–594, Jun. 1993.
[47] B. Chamadiya, K. Mankodiya, M. Wagner, and U. G. Hofmann, "Textile-based, contactless ECG monitoring for non-ICU clinical settings," *J. Ambient Intell. Humaniz. Comput.*, vol. 4, no. 6, pp. 791–800, Dec. 2013.
[48] M. Y. M. Wong, E. P. MacPherson, and Y. T. Zhang, "Contactless and continuous monitoring of heart rate based on photoplethysmography on a mattress," *Physiol. Meas.*, vol. 31, no. 7, p. 1065, 2010.
[49] K. Humphreys, T. Ward, and C. Markham, "Noncontact simultaneous dual wavelength photoplethysmography: A further step toward noncontact pulse oximetry," *Rev. Sci. Instrum.*, vol. 78, no. 4, Apr. 2007, Art. no. 044304.
[50] M.-Z. Poh, D. J. McDuff, and R. W. Picard, "Non-contact, automated cardiac pulse measurements using video imaging and blind source separation," *Opt. Express*, vol. 18, no. 10, pp. 10762–10774, 2010.
[51] Y. Sun, S. Hu, V. Azorin-Peris, S. Greenwald, J. Chambers, and Y. Zhu, "Motion-compensated noncontact imaging photoplethysmography to monitor cardiorespiratory status during exercise," *J. Biomed. Opt.*, vol. 16, no. 7, 2011, Art. no. 077010.
[52] M.-Z. Poh, D. J. McDuff, and R. W. Picard, "Advancements in noncontact, multiparameter physiological measurements using a webcam," *IEEE Trans. Biomed. Eng.*, vol. 58, no. 1, pp. 7–11, Jan. 2011.
[53] L. Kong *et al.*, "Non-contact detection of oxygen saturation based on visible light imaging device using ambient light," *Opt. Express*, vol. 21, no. 15, pp. 17464–17471, 2013.
[54] U. S. Freitas, "Remote camera-based pulse oximetry," in *Proc. 6th Int. Conf. eHealth, Telemedicine, Social Med. (eTELEMED)*, 2014, pp. 59–63.
[55] A. Aubert *et al.*, "Laser method for recording displacement of the heart and chest wall," *Med. Eng. Phys.*, vol. 6, no. 2, pp. 134–140, 1984.
[56] H. Hong and M. D. Fox, "Noninvasive detection of cardiovascular pulsations by optical Doppler techniques," *Proc. SPIE*, vol. 2, no. 4, pp. 382–391, 1997.
[57] C. C. Wang *et al.*, "Human life signs detection using high-sensitivity pulsed laser vibrometer," *IEEE Sensors J.*, vol. 7, no. 9, pp. 1370–1376, Sep. 2007.
[58] S. Casaccia, E. J. Sirevaag, E. Richter, J. A. O'Sullivan, L. Scalise, and J. W. Rohrbaugh, "Decoding carotid pressure waveforms recorded by laser Doppler vibrometry: Effects of rebreathing," in *Proc. AIP Conf.*, vol. 1600, no. 1, 2014, pp. 298–312.
[59] S. Casaccia, "Measurement of physiological parameters in the human body by non-contact technique: Laser Doppler vibrometry," Ph.D. dissertation, Università Politecnica delle Marche, Ancona, Italy, 2015.
[60] U. Morbiducci, L. Scalise, M. De Melis, and M. Grigioni, "Optical vibrocardiography: A novel tool for the optical monitoring of cardiac activity," *Ann. Biomed. Eng.*, vol. 35, no. 1, pp. 45–58, Jan. 2007.
[61] I. Fujimasa, T. Chinzei, and I. Saito, "Converting far infrared image information to other physiological data," *IEEE Eng. Med. Biol. Mag.*, vol. 19, no. 3, pp. 71–76, May 2000.
[62] I. Pavlidis and J. Levine, "Thermal image analysis for polygraph testing," *IEEE Eng. Med. Biol. Mag.*, vol. 21, no. 6, pp. 56–64, Nov. 2002.
[63] M. Garbey, N. Sun, A. Merla, and I. Pavlidis, "Contact-free measurement of cardiac pulse based on the analysis of thermal imagery," *IEEE Trans. Biomed. Eng.*, vol. 54, no. 8, pp. 1418–1426, Aug. 2007.
[64] L. Zhou, M. Yin, X. Xu, X. Yuan, and X. Liu, "Non-contact detection of human heart rate with kinect," *Cluster Comput.*, pp. 1–8, Jan. 2018.
[65] K. Nakajima, T. Maekawa, and H. Miike, "Detection of apparent skin motion using optical flow analysis: Blood pulsation signal obtained from optical flow sequence," *Rev. Sci. Instrum.*, vol. 68, no. 2, pp. 1331–1336, 1997.
[66] A. Al-Naji and J. Chahl, "Remote optical cardiopulmonary signal extraction with noise artifact removal, multiple subject detection & long-distance," *IEEE Access*, vol. 6, pp. 11573–11595, 2018.
[67] R. Vas, C. R. Joyner, D. E. Pittman, and T. C. Gay, "The displacement cardiograph," *IEEE Trans. Biomed. Eng.*, vol. BME-23, no. 1, pp. 49–54, Jan. 1976.
[68] D. L. Wilson and D. B. Geselowitz, "Physical principles of the displacement cardiograph including a new device sensitive to variations in torso resistivity," *IEEE Trans. Biomed. Eng.*, vol. BME-28, no. 10, pp. 702–710, Oct. 1981.
[69] R. Guardo, S. Trudelle, A. Adler, C. Boulay, and P. Savard, "Contactless recording of cardiac related thoracic conductivity changes," in *Proc. 17th Int. Conf. Eng. Med. Biol. Soc.*, vol. 2, 1995, pp. 1581–1582.
[70] F. Liebold, M. Hamsch, and C. Igney, "Contact-less human vital sign monitoring with a 12 channel synchronous parallel processing magnetic impedance measurement system," in *Proc. 4th Eur. Conf. Int. Fed. Med. Biol. Eng.* Berlin, Germany: Springer, 2009, pp. 1070–1073.
[71] A. Cordes, J. Foussier, D. Pollig, and S. Leonhardt, "A portable magnetic induction measurement system (PIMS)," *Biomedizinische Technik/Biomed. Eng.*, vol. 57, no. 2, pp. 131–138, 2012.
[72] C. Brüser, C. H. Antink, T. Wartzek, M. Walter, and S. Leonhardt, "Ambient and unobtrusive cardiorespiratory monitoring techniques," *IEEE Rev. Biomed. Eng.*, vol. 8, pp. 30–43, 2015.

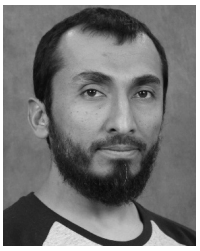

AHMAD SULIMAN (S'14) received the B.S. degree in electrical and electronics engineering from Kabul University, Kabul, in 2003, and the M.S. degree in electrical and computer engineering with a focus on embedded systems and controls from Kansas State University (KSU), Manhattan, KS, USA, in 2010, where he is currently pursuing the Ph.D. degree in electrical engineering with a focus on biomedical devices.

From 2004 to 2008, he involved in mobile telecommunication systems with the Siemens AG Telecommunications Department local branch, Kabul. From 2011 to 2014, he was a Lecturer with Kabul University, where he taught several senior level courses in electrical engineering. From 2014 to 2017, he was a Graduate Research Assistant with the KSU Medical Component Design Laboratory and the Brain and Body Sensing Laboratory. His research interests include analog and digital signal processing in low frequency signal applications, particularly biomedical signals, low-noise circuit design, and systems engineering for unobtrusive biomedical applications.

Dr. Suliman is a member of the IEEE Engineering in Medicine and Biology Society.

CHARLES CARLSON (S'14) received the B.S. degree in physics from Fort Hays State University, in 2013, and the B.S. and M.S. degrees in electrical engineering from Kansas State University (KSU), in 2013 and 2015, respectively, where he is currently pursuing the Ph.D. degree in electrical engineering.

He is currently a Graduate Teaching and Research Assistant in electrical and computer engineering with the KSU. He is also with the KSU Medical Component Design Laboratory and is interested in engineering education, biotechnology, and bioinstrumentation.

Mr. Carlson is a member of the American Society for Engineering Education and the IEEE Engineering in Medicine and Biology Society.

CARL J. ADE received the B.S. degree in biology from Kansas Wesleyan University, in 2004, and the M.S. degree in Kinesiology and the Ph.D. degree in Anatomy and Physiology from Kansas State University, in 2008 and 2013, respectively.

He is currently an Assistant Professor with the Department of Kinesiology, Kansas State University. He directs the Clinical Integrative Physiology Laboratory, a National Institutes of Health and National Aeronautics and Space Administration funded research and teaching facility focused primary on understanding the development of heart failure and cardiovascular disease associated with cancer-associated treatments (i.e, chemotherapy, immunotherapy, hormone deprivation, and radiation), and the cardiovascular consequences of long-duration spaceflight.

STEVE WARREN received the B.S. and M.S. degrees in electrical engineering from Kansas State University, in 1989 and 1991, respectively, and the Ph.D. degree in electrical engineering from The University of Texas at Austin, in 1994.

He is currently a Professor with the Department of Electrical and Computer Engineering, Kansas State University. He directs the Medical Component Design Laboratory, a National Science Foundation funded research and teaching facility that supports the development of health monitoring technologies. His researches focus on (1) plug-and-play, point-of-care health systems that use interoperability standards, and (2) wearable sensors and signal processing techniques to determine human and animal well-being.

Dr. Warren is a member of the American Society for Engineering Education and the Institute of Electrical and Electronics Engineers. He serves as the Faculty Advisor for the KSU Student Chapter of the IEEE Engineering in Medicine and Biology Society, and he is the Program Coordinator for the KSU undergraduate degree in biomedical engineering.

DAVID E. THOMPSON (S'06–M'13) received the B.S. degree in electrical engineering from Kansas State University, in 2006, and the M.S. degree in biomedical engineering, the M.S.E. degree in electrical engineering: systems, and the Ph.D. degree in biomedical engineering from the University of Michigan, Ann Arbor, in 2009, 2011, and 2012, respectively.

From 2012 to 2013, he was a Postdoctoral Research Fellow at the University of Michigan. In 2014, he became an Assistant Professor of electrical and computer engineering at Kansas State University. He has authored sixteen full-length scientific articles. His research interests include brain-computer interfaces, performance measurement, and non-invasive sensing. He was a founding member of the Brain-Computer Interface Society. At Kansas State, he founded the Brain and Body Sensing Laboratory. He was a Goldwater Scholar, Fulbright Fellow to Japan, and National Science Foundation Graduate Research Fellow.